

## RESEARCH OUTPUTS / RÉSULTATS DE RECHERCHE

### Photoluminescence properties and quantum size effect of ZnO nanoparticles confined inside a faujasite X zeolite matrix

Bouvy, Claire; Marine, Wladimir; Sporcken, Robert; Su, Bao-Lian

*Published in:*  
Chemical Physics Letters

*Publication date:*  
2006

*Document Version*  
Early version, also known as pre-print

[Link to publication](#)

*Citation for published version (HARVARD):*  
Bouvy, C, Marine, W, Sporcken, R & Su, B-L 2006, 'Photoluminescence properties and quantum size effect of ZnO nanoparticles confined inside a faujasite X zeolite matrix', *Chemical Physics Letters*, vol. 428, no. 4-6, pp. 312-316.

#### General rights

Copyright and moral rights for the publications made accessible in the public portal are retained by the authors and/or other copyright owners and it is a condition of accessing publications that users recognise and abide by the legal requirements associated with these rights.

- Users may download and print one copy of any publication from the public portal for the purpose of private study or research.
- You may not further distribute the material or use it for any profit-making activity or commercial gain
- You may freely distribute the URL identifying the publication in the public portal ?

#### Take down policy

If you believe that this document breaches copyright please contact us providing details, and we will remove access to the work immediately and investigate your claim.

# Photoluminescence properties and quantum size effect of ZnO nanoparticles confined inside a faujasite X zeolite matrix

C. Bouvy <sup>a,1</sup>, W. Marine <sup>b</sup>, R. Sporcken <sup>c</sup>, B.L. Su <sup>a,\*</sup>

<sup>a</sup> *Laboratoire de Chimie des Matériaux Inorganiques (CMI), The University of Namur (FUNDP), Rue de Bruxelles 61, B-5000 Namur, Belgium*

<sup>b</sup> *CRMCN, UMR CNRS 6631, Département de Physique, Case 901, Faculté des Sciences de Luminy, Université de la Méditerranée, F-13288 Marseille, Cedex 9, France*

<sup>c</sup> *Laboratoire de Physique des Matériaux Electroniques (LPME), The University of Namur (FUNDP), Rue de Bruxelles 61, B-5000 Namur, Belgium*

Received 30 March 2006; in final form 26 June 2006

Available online 5 July 2006

## Abstract

ZnO nanoparticles were grown inside a faujasite matrix by wet chemistry method. The structural and textural results by N<sub>2</sub> adsorption, X-ray diffraction, <sup>29</sup>Si and <sup>27</sup>Al solid state NMR indicated successful incorporation of ZnO nanoparticles inside supercages of zeolite. After the incorporation, a slight structural symmetry change of the zeolite occurred. The photoluminescence of ZnO nanoparticles in zeolite matrix was studied by exciting the sample with an ArF laser (193 nm). A strong blue-shift of the emission band of ZnO, suggesting a strong quantum size effect, is observed. It is also revealed an improved stability of excitons when ZnO nanoparticles are confined within a zeolite matrix.

© 2006 Elsevier B.V. All rights reserved.

## 1. Introduction

The preparation of light-emitting nanostructures based on semiconducting materials of nanometer scale has recently received considerable attention because of the unique optoelectronic properties appearing in this size range. In particular, Zinc Oxide, a wide band-gap II–VI semiconductor (gap = 3.37 eV, 298 K), shows significant quantum confinement effect (QSE) when its size reaches the Bohr radius, *ca.* 1.8 nm. Moreover, ZnO is an interesting material due to its many applications such as varistors [1,2], gas sensors [3,4], ceramics [5], electrical and optical devices [6,7] and exhibits photoluminescence gain and lasing effect. However, the threshold for lasing was very high [8] and only low-dimensional nanostructures can facilitate lasing.

Various methods have been employed to prepare ZnO nanoparticles with extremely small diameters including

precipitation of colloids in solution [9], sol–gel methods [10], thermal decomposition methods [11], pulsed laser deposition (PLD) [12] and metal-organic chemical vapour deposition (MOCVD) [13]. However, in general it is very difficult to avoid the aggregation of ZnO nanoparticles during the preparation. This work aims to resolve this problem via the growth of ZnO nanoparticles inside the channels of a porous matrix. The faujasite X zeolite, with 3D channels connected by supercages of 1.3 nm in diameter, was employed for the conception of ZnO/faujasite nanocomposites. The photoluminescence properties of the nanocomposites have been evaluated and the optical character of the nanocomposites has been correlated with the particle size of ZnO.

## 2. Experimental

### 2.1. Nanocomposite preparation

Faujasite X zeolite was synthesized by stirring a sodium aluminate solution with a mixture of NaOH and KOH dissolved in distilled water. After homogenisation, an aqueous

\* Corresponding author. Fax: +32 81 72 54 14.

E-mail address: [bao-lian.su@fundp.ac.be](mailto:bao-lian.su@fundp.ac.be) (B.L. Su).

<sup>1</sup> FRIA fellow (Fonds National de la Recherche Scientifique, rue d'Egmont 5, B-1000 Bruxelles, Belgium).

sodium silicate solution was rapidly added to the mixture under strong agitation in a molar ratio  $\text{SiO}_2/\text{Al}_2\text{O}_3 = 2.2$ . The resulting gel was aged at 70 °C for 24 h before washing and drying. On the basis of the chemical analysis made by Atomic absorption spectrometry, the as-prepared zeolite, labelled here FAU, had a Si/Al ratio of 1 with a chemical composition of  $\text{Na}_{62}\text{K}_{34}\text{Si}_{96}\text{Al}_{96}\text{O}_{192}$ .

The incorporation of ZnO was performed by impregnation of 0.5 g FAU into 20 ml of a 1 M  $\text{Zn}(\text{NO}_3)_2$  aqueous solution over 20 min. The powder was separated by centrifugation, was dried and calcined under flowing  $\text{O}_2$  for 6 h at 550 °C. The obtained powder is labelled ZnO/FAU. The chemical analysis gives 36.2 wt% of ZnO impregnated in faujasite zeolite, i.e. 0.362 g of ZnO for 1 g of zeolite.

## 2.2. Characterization

Nitrogen adsorption–desorption isotherms were measured at 77 K on a Micromeritics ASAP 2010 instrument. The samples were first degassed under vacuum at 593 K for several hours. The Horvath–Kawazoe [14] method was used for pore size estimation. The surface areas were determined using the BET equation in the low pressure region ( $0.05 \leq p/p_0 \leq 0.25$ ). X-ray diffraction (XRD) patterns were recorded on a Philips PW1820 diffractometer using Cu K $\alpha$  radiation with wavelength of 1.54178 Å. Solid state magic angle spinning (MAS)-NMR spectra were obtained with a Bruker MSL 500 spectrometer for  $^{29}\text{Si}$  (at 99.25 MHz) and a Bruker MSL 400 spectrometer for  $^{27}\text{Al}$  (at 104.3 MHz). Photoluminescence spectra were recorded at room temperature with an ArF laser (193 nm) as the excitation source and an iCCD camera as the detector. The laser beam was focused onto the sample with a spot size of  $1.36 \times 10^{-2} \text{ cm}^2$ . For the time-resolved luminescence spectra, the excitation was made by the ArF laser with a repetition rate of 5 Hz and pulse duration of 8 ns. The iCCD camera gate width was 5 ns and the decay curve was measured from the maximum intensity of the ZnO PL band until its extinction at room temperature.

## 3. Results and discussion

Nitrogen adsorption–desorption results (Table 1 and Fig. 1) indicate that microporosity is well maintained after incorporation of ZnO and the decrease in specific area confirms the introduction of ZnO inside the channels. At the same time, the mean pore diameter is not affected by the presence of ZnO nanoparticles inside the structure.

As the decrease in microporous area is more significant than the total specific area (including the external surface) it is possible that the majority of the nanoparticles are confined within the structure of the zeolite. On the other hand, both samples exhibit a hysteresis loop at relatively high relative pressure due to capillary condensation effects, generally associated with the creation of mesopores [15,16]. The presence of the mesoporosity can lead to the formation of ZnO nanoparticles larger than the size of supercages (1.3 nm).

Powder X-ray diffraction patterns of the parent zeolite FAU and the ZnO/FAU nanocomposite are shown in Fig. 2. For a better understanding, the XRD pattern of commercial ZnO is also shown. It can clearly be seen that the pattern of FAU and ZnO/FAU are somehow different thus indicating some changes in the crystalline structure of FAU. Change of the relative peaks intensity and small shift of the diffraction angles to the higher values indicate the compression of the FAU crystalline structure in the presence of ZnO. It is observed that the first diffraction line (111) at  $6.15^\circ$  ( $2\theta$ ) is sharply increased in intensity while some other diffraction lines such as (220) at  $10.11^\circ$  ( $2\theta$ ), (311) at  $11.86^\circ$  ( $2\theta$ ) decrease significantly their intensity after incorporation of ZnO nanoparticles. This phenomenon is often observed in Na form faujasite zeolites after ion exchange with bivalent cations like  $\text{Ca}^{2+}$  since the introduction of bivalent  $\text{Ca}^{2+}$  ions to replace monovalent  $\text{Na}^+$  ions (one  $\text{Ca}^{2+}$  for  $\text{Na}^+$  ions) will change the symmetry of crystalline structure from Fd3 (Na-FAU) to Fd3m (NaCa-FAU) [17]. This indicates that the formation of

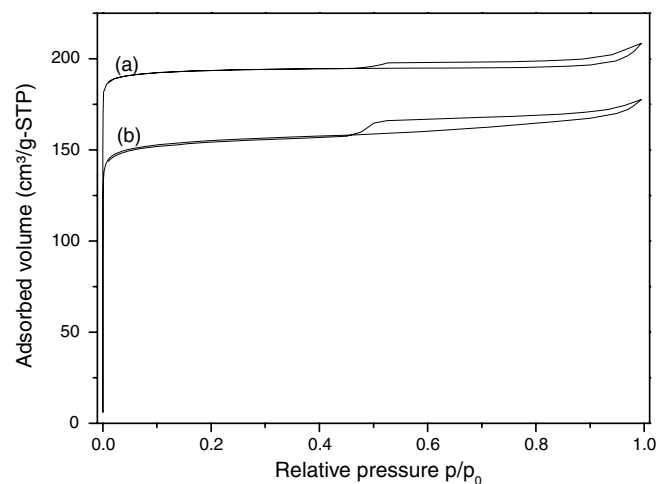


Fig. 1. Nitrogen adsorption–desorption isotherms of: (a) faujasite X matrix (b) ZnO/FAU nanocomposite.

Table 1  
Textural properties of the FAU X zeolite and the ZnO/FAU nanocomposite

	Specific area ( $\text{m}^2/\text{g}$ )	Pore volume ( $\text{cm}^3/\text{g}$ )	Pore diameter (Å)	Microporous area ( $\text{m}^2/\text{g}$ )	Microporous volume ( $\text{cm}^3/\text{g}$ )
FAU	616	0.32	5.0	594	0.30
ZnO/FAU	497	0.27	5.0	451	0.22
Variation (%)	19	16		27	24

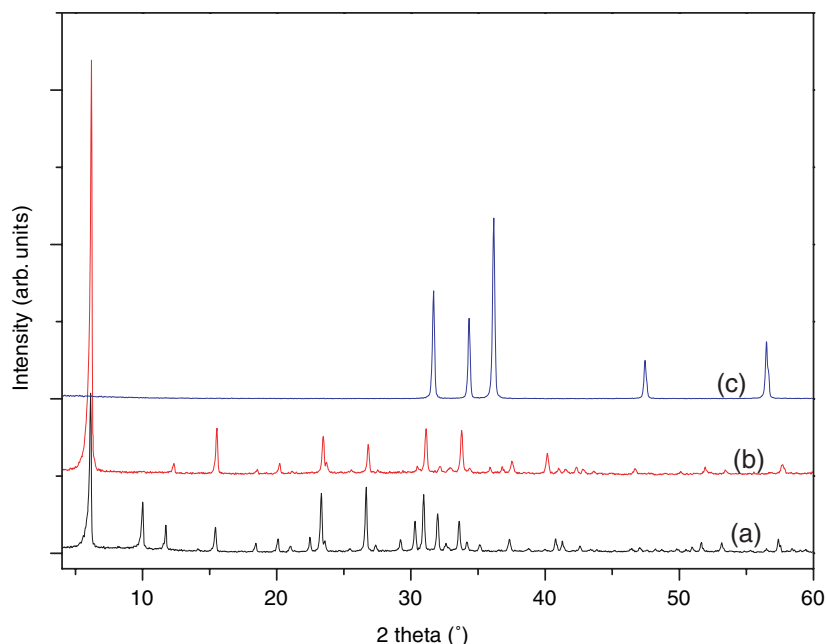


Fig. 2. Powder XRD patterns of: (a) faujasite X zeolite matrix, (b) ZnO-FAU, and (c) commercial ZnO.

ZnO nanoparticles in faujasite zeolite will change the symmetry of the system. It is also possible that ion exchange can occur and some  $\text{Zn}^{2+}$  ions replace  $\text{Na}^{+}$  ions to play the role of the compensating ions.

However no ZnO peaks can be observed in the XRD pattern of ZnO/FAU thus meaning that no big particles were formed both inside and outside the zeolite framework during the growth process in confirmation with the nitrogen adsorption–desorption results. In order to gain a deeper understanding of the structural changes observed within the faujasite crystallites after the incorporation of ZnO,  $^{29}\text{Si}$  and  $^{27}\text{Al}$  NMR were performed (Fig. 3 and Table 2).

For the  $^{29}\text{Si}$  NMR spectra the signal at  $-84$  ppm was assigned to Si atoms with 4 Al neighbours while for the  $^{27}\text{Al}$  NMR spectra, the resonance centred around 60 ppm represents tetrahedrally coordinated Al. In both cases, except for the small shift of the signal position, an important broadening of the bands is observed. This broadening can be explained by the interaction created between the ZnO nanoparticles and the FAU internal surface and also by the symmetrical changes observed in the XRD patterns. These observations led to a preliminary conclusion that during the growth of ZnO nanoparticles inside the faujasite, textural properties were conserved and that some symmetrical changes did occur but without the collapse of the zeolite framework. From this, it can be affirmed that the growth of the nanoparticles has been well limited by the zeolite walls.

PL results at room temperature are presented in Fig. 4. First, the emission spectrum of the faujasite zeolite matrix (Fig. 4a) under excitation at 193 nm (6.4 eV) is composed of one broad band around 4.18 eV and one smaller band at 3.26 eV. The origin of this weak photoluminescence is

still unknown owing to an absence of information on the optical properties of zeolites within the literature. The emission spectrum of the nanocomposite is presented in Fig. 4b. A very broad PL band can be seen between 2.75 and 4.75 eV. The contribution to the band by the matrix has either vanished or is hidden by the very intense photoluminescence of ZnO/FAU. Two Gaussian functions are obtained by fitting the emission spectrum. The results are given in Table 3.

The obtained values of 3.62 and 3.98 eV, which are much higher than that of bulky ZnO (3.37 eV), can be attributed to ZnO nanoparticles with two different sizes. Using the equation based on the effective mass approximation given by Brus in 1984 [18] a particle size of 1.7 nm (for the PL at 3.98 eV) and 2.5 nm (for 3.62 eV) has been determined. It is believed that these values are an approximation and do not correspond exactly with the real particle size. This inaccuracy could be due to the use of values that were determined for bulk ZnO and not for nanosized ZnO, such as the effective masses and the optical dielectric constant. However, on the basis of the results obtained, it is suggested that some particles have grown inside the supercages and give rise to the strongest quantum size effect whilst other particles have continued to grow by the expansion of zeolite framework, inducing a change in structural symmetry and thus yielding a smaller QSE. It is also possible that these larger particles could be formed in mesopores as shown by  $\text{N}_2$  adsorption isotherms the presence of mesopore type hysteresis loop (Fig. 1).

Fig. 5 illustrates a time-resolved photoluminescence spectrum of the emission of ZnO nanoparticles. The intensity of the luminescence band decreases with time. This decay can be fitted to the exponential curve ( $y = A \cdot \exp(-t/\tau)$ ), with  $\tau = 8.93$  ns. This value is rather high in compar-

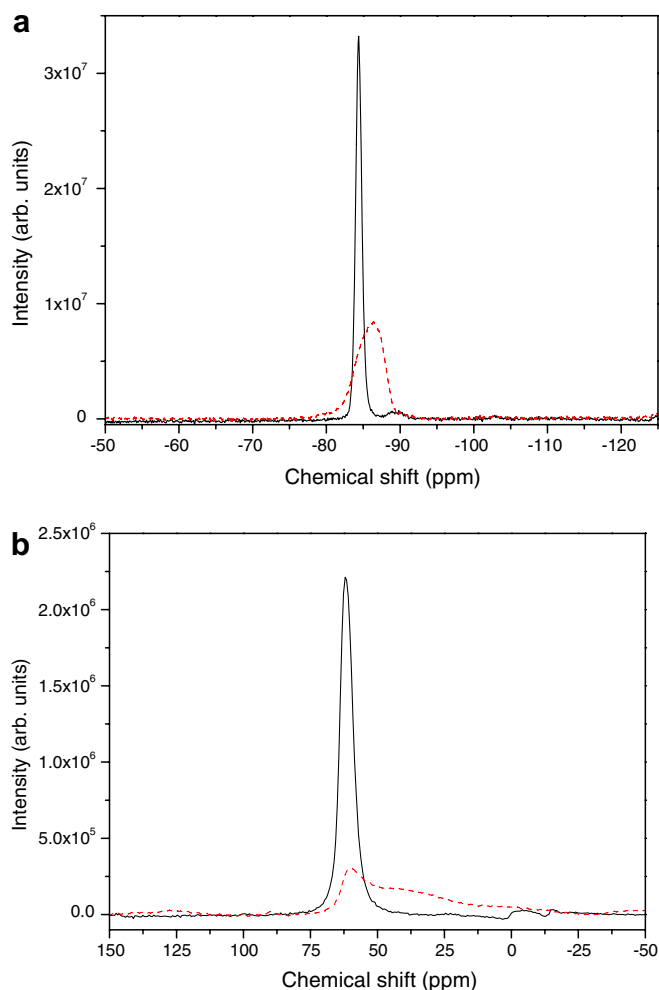


Fig. 3. (a)  $^{29}\text{Si}$  NMR spectra of FAU (solid line) and ZnO-FAU (dashed line) (b)  $^{27}\text{Al}$  NMR spectra of FAU (solid line) and ZnO-FAU (dashed line).

Table 2

Chemical shifts and widths of the NMR bands of FAU X zeolite and ZnO-FAU nanocomposite

FAU	$^{29}\text{Si}$ (ppm)		$^{27}\text{Al}$ (ppm)	
	Chemical shift	FWHM	Chemical shift	FWHM
	-84	0.95	63	5.5
ZnO-FAU	-86	4.5	60 (+39)	7.5

ison to those reported in the literature [19–21], indicating the improved stability of excitons when the ZnO nanoparticles are confined within a zeolite matrix.

#### 4. Conclusions

Zeolite framework is efficient matrix to control the growth of ZnO nanoparticles. Nitrogen adsorption-desorption results reveal no important changes in the textural properties of the zeolite after the incorporation process. The presence of ZnO in zeolite changes the structural symmetry. PL results

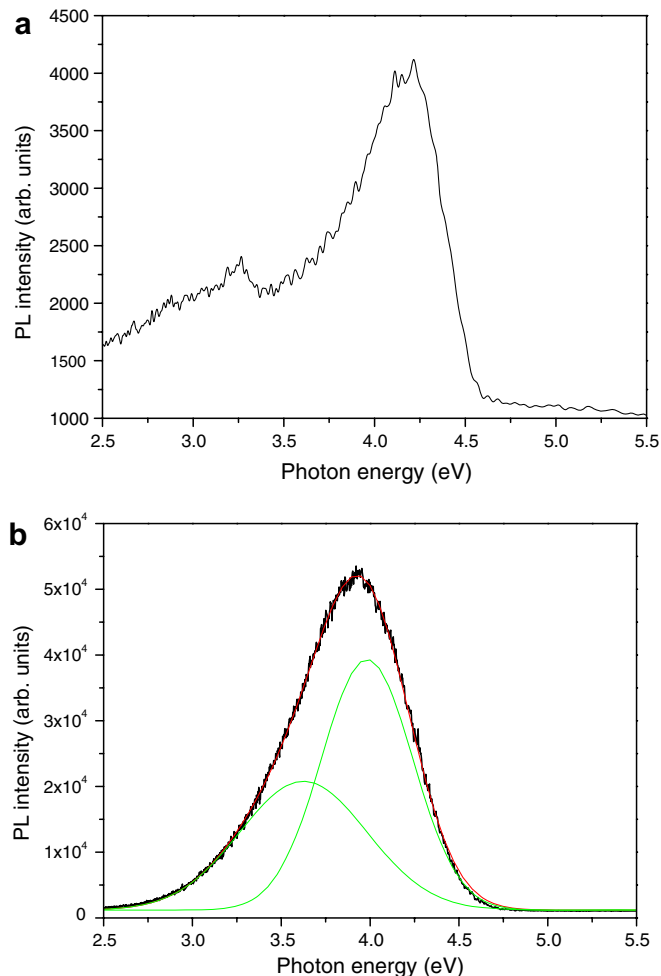


Fig. 4. PL spectra of the FAU X zeolite (a) and the ZnO-FAU nanocomposite (b) ( $E_{\text{exc}} = 6.4$  eV).

Table 3

Results of the GAUSSIAN decomposition of the PL spectrum of the ZnO/FAU nanocomposite

	Wavelength (eV)	FWHM (eV)
Peak 1	3.62	0.72
Peak 2	3.98	0.51

show an important blue-shift of the ZnO emission band, which is attributed to the quantum size effect due to the size of the ZnO nanoparticles formed inside the zeolite. An improved stability of excitons is obtained by the confinement of ZnO nanoparticles within a microporous zeolite matrix. Our next step is to tailor and to homogenize the particle size of ZnO in different porous matrix to design the light-emitting systems and laser generators.

#### Acknowledgements

C. Bouvy thanks the FRIA (Fonds National de la Recherche Scientifique) for a doctoral fellowship. This work was realized in the frame of Belgian federal government project

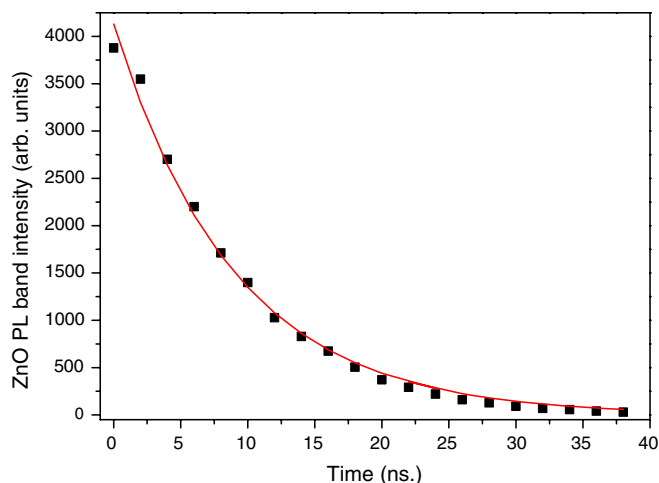


Fig. 5. Time-resolved photoluminescence decay of the ZnO PL band (points represent the experimental data and the line the exponential fit).

PAI/IUAP 5/01. Financial supports from the University of Namur (FUNDP) and from the European SOXESS network were gratefully acknowledged.

## References

- [1] D.R. Clarke, *Journal of American Ceramic Society* 82 (1999) 485.
- [2] N.T. Hung, N.D. Quang, S. Bernik, *Journal of Material Research* 16 (2001) 2817.
- [3] Y. Shimizu, F.C. Lin, Y. Takao, M. Egashira, *Journal of American Ceramic Society* 81 (1998) 1633.
- [4] R. Paneva, D. Gotchev, *Sensors and Actuator A: Physical* 72 (1999) 79.
- [5] L. Gao, Q. Li, W.L. Luan, *Journal of American Ceramic Society* 85 (2002) 1016.
- [6] B.D. Yao, H.Z. Shi, H.J. Bi, L.D. Zhang, *Journal of Physics: Condensed Matter* 12 (2000) 6265.
- [7] Y.C. Kong, D.P. Yu, B. Zhang, W. Fang, S.Q. Feng, *Applied Physics Letters* 78 (2001) 407.
- [8] J.C. Johnson, H. Yan, R.D. Schaller, L.H. Haber, R.J. Saykally, P.D. Yang, *Journal of Physical Chemistry B* 105 (2001) 11387.
- [9] U. Koch, A. Fojtik, H. Weller, A. Henglein, *Chemical Physics Letters* 122 (1985) 507.
- [10] C. Cannas, M. Casu, A. Lai, A. Musinu, G. Piccaluga, *Journal of Materials Chemistry* 9 (1999) 1765.
- [11] L. Jing, Z. Xu, J. Shang, X. Sun, W. Cai, H. Guo, *Materials Science and Engineering A* 332 (2002) 356.
- [12] I. Ozerov, D. Nelson, A.V. Bulgakov, W. Marine, M. Sentis, *Applied Surface Science* 9789 (2003) 1.
- [13] B. Hahn, G. Heindel, E. Pschoor-Schoberer, W. Gebhardt, *Semiconductor Science and Technology* 13 (1998) 788.
- [14] G. Hortvath, K.J. Kawazoe, *Journal of Chemical Engineering of Japan* 16 (1983) 470.
- [15] J. Rathousky, A. Zukal, N. Jaeger, G. Schulz-Ekloff, *Journal of Chemical Society, Faraday Transactions* 88 (1992) 489.
- [16] M. Wark, H. Kessler, G. Schulz-Ekloff, *Microporous Materials* 8 (1997) 241.
- [17] M.M.J. Treacy, J.B. Higgins, *Collections of Simulated XRD Powder Patterns for Zeolites*, Elsevier, Amsterdam, 2001.
- [18] L.E. Brus, *Journal of Chemical Physics* 80 (1984) 4403.
- [19] T. Hirai, Y. Harada, S. Hashimoto, K. Edamatsu, T. Itoh, *Journal of Luminescence* 94–95 (2001) 261.
- [20] B. Guo, Z. Ye, K.S. Wong, *Journal of Crystal Growth* 253 (2003) 252.
- [21] T. Hirai, Y. Harada, S. Hashimoto, T. Itoh, N. Ohno, *Journal of Luminescence* 112 (2005) 196.